

Diode-pumped, non-resonant, continuous-wave Raman laser in H₂ using resonant optical feedback stabilization**P. A. Roos, J. K. Brasseur, and J. L. Carlsten***Montana State University, Department of Physics, Bozeman, MT 59717**roos@physics.montana.edu, brasseur@physics.montana.edu, carlsten@physics.montana.edu*

We demonstrate a non-resonant cw Raman laser pumped by an optically-locked diode laser at 790nm which produces cw Stokes (1178nm) and coherent anti-Stokes (595nm) emission. Considering the modest pump powers, relative low cost, and predicted spectral purity, frequency down-conversion of tunable diode lasers via stimulated Raman scattering will provide attractive sources for remote sensing, spectroscopic, and atomic physics applications. Stokes laser threshold is $240 \pm 19 \mu\text{W}$ pump power and emission is observed over a range of roughly 10nm by adjusting the optical locking feedback phase. Photon conversion efficiency rises throughout the pump power region studied with a peak value of $15 \pm 2\%$.

Diode-pumped, non-resonant, continuous-wave Raman laser in H₂ using resonant optical feedback stabilization

P. A. Roos, J. K. Brasseur, and J. L. Carlsten

Montana State University, Department of Physics, Bozeman, MT 59717

roos@physics.montana.edu, brasseur@physics.montana.edu, carlsten@physics.montana.edu

Historically, non-resonant stimulated Raman scattering (SRS) in gases has been limited to the pulsed laser regime due to the high (>100kW) pump powers required for the nonlinear process to occur[1]. However, Brasseur et. al. recently Raman-shifted the frequency of a highly stabilized cw Nd:YAG laser at 532nm to produce cw Stokes laser output at 683nm in H₂ with milliwatt pump and output powers[2,3]. This was achieved by placing the Raman active medium between the mirrors of a high finesse Fabry-Perot cavity (HFC). By high-reflective (HR) coating the HFC mirrors for both the pump and Stokes wavelengths, substantial optical power build up within the optical cavity compensated for the low Raman gain far off resonance. However, the allure of such frequency conversion is perhaps most prominent in the diode laser regime due to their broad spectral coverage and tunability. With the added benefits of modest pump powers and relative low cost as well as high spatial quality and predicted spectral purity, Raman-shifted tunable diode lasers are promising sources for spectroscopic applications. We report, to our knowledge, the first cw Stokes and coherent anti-Stokes emission from a non-resonant Raman laser pumped by a tunable diode laser source.

The particular vibrational Raman process utilized for this work is discussed in references 2 and 3 with the proper wavelength substitutions ($\lambda_{\text{Pump}} = 790\text{nm}$, $\lambda_{\text{Stokes}} = 1178\text{nm}$). Although other cw Raman lasers have previously been achieved, their spectral coverage and tunability were limited to narrow regions near molecular or atomic resonances in order to maximize the

Raman gain [4,5,6]. In the present work, we pump the Raman active medium far off resonance, in the relatively flat region of the Raman gain [7]. This allows broad wavelength tunability with minimal change in laser output power. At 790nm, tuning over 20nm will produce just ~4% change in the Raman gain. To compensate for the low gain in this region, we place the Raman active medium in a HFC. By locking the laser frequency to a resonance of this cavity, sufficient pump power can build within the cavity to achieve SRS with milliwatt-range external pump power.

In this work, we not only use the HFC to build sufficient optical power for SRS, but we also use resonant optical feedback from the cavity to narrow the laser's spectral width and to lock its center frequency to a HFC resonance [8-12]. The scheme employed is similar to that first demonstrated by Dahmani and coworkers [8]. However, the present design differs from past work in two notable respects. First, as depicted conceptually in figure 1, the optical feedback path can be viewed as a ring rather than a linear reflection. This slightly modifies the theory presented in the references and allows independent attenuation of the feedback level. As will be shown in the next figure, the beam splitting mechanism corresponds to the output isolator of an optical isolator. This allows energy circulation in only the clockwise direction around the ring in figure 1, as denoted by the arrows. Second, the finesse of the cavity used in this experiment is substantially greater than that used in previous resonant feedback locking. Although the laser locks to a single HFC mode, it also exhibits stable locking for other HFC modes without changing the drive current. Furthermore, stable locking is observed for all drive currents.

As depicted in Figure 2, a HFC filled with H₂ is pumped by a free running diode laser at 790nm. The laser source is a temperature stabilized, 100mW Fabry-Perot type device with ~4% front facet reflectivity. A Faraday isolator attenuates non-resonant reflected light by ~35dB. A

half-wave plate and polarizer are used in tandem as a variable attenuator for the pump. Mirror M_1 is reflective coated only for the pump thereby allowing transmission of Stokes (1178nm) and anti-Stokes (595nm). The HFC consists of two curved mirrors of radii ± 50 cm, separated by 7.62cm, and HR coated for both the pump and Stokes wavelengths. Using the manufacturer quoted reflectivities, the finesse at both wavelengths is roughly 60,000. The HFC is enclosed within a hermetically sealed container filled with 10atm of diatomic hydrogen gas. Cavity transmission is fed back to the diode laser via the output polarizer of the Faraday isolator. The feedback power can be adjusted using another half-wave plate in the transmission leg before the isolator polarizer. Assuming lossless coupling back into the diode cavity mode, the ratio of optical feedback power to the laser diode emission power is $\sim 10^{-3}$ for the data presented in this paper.

Due to the phase dependence of the optical locking, the HFC mirror separation is electronically servoed providing further stabilization via the Pound-Drever-Hall method [13]. Stable locking is also observed by controlling mirror M_3 . An electrooptic modulator (EOM) places 10 MHz sidebands on the carrier frequency to produce an error signal for electronic locking. A 75-25 beam splitter is used to divert a portion of the reflected field from the front of the HFC in order to detect an error signal.

Figure 3 shows transmitted pump and Stokes optical powers as functions of input pump optical power. The bottom axis accounts for coupling losses into the HFC while the top axis gives the pump power directly outside the cavity. The solid lines represent theoretical models developed in references 3 and 14 using the following parameters: $\lambda_p=790$ nm, $\lambda_s=1178$ nm, $\alpha=1.62 \times 10^{-9}$ cm/W, $\ell=7.62$ cm, $R_p=0.99993$, $R_s=0.999948$, $T_p=58$ ppm, $T_s=22$ ppm, $b=26.5$ cm. The manufacturer quoted mirror reflectivities are 0.99995 for both the pump and Stokes. The

plane-wave gain coefficient, α , was calculated from reference 7. The transmitted pump increases linearly until Stokes laser threshold at $240 \pm 19 \mu\text{W}$, at which point the transmitted pump power abruptly levels off as predicted. The error in this value comes mostly from uncertainty in the coupling efficiency into the fundamental cavity mode as a result of uncertain mirror reflectivities. To our knowledge, this is the lowest cw Raman laser threshold yet observed.

The reflectivities of the mirrors used in this experiment were selected to minimize the Stokes laser threshold and therefore do not optimize photon conversion efficiency. Figure 4 shows the measured and predicted photon conversion efficiencies from the pump to the Stokes beams as a function of pump power. The maximum conversion efficiency observed is $15 \pm 2\%$, but is predicted to reach a peak value over 17% at four times threshold pump power. Efficiencies approaching 100% are predicted using appropriate mirrors reflectivities [15]. Stokes emission polarization matches that of the pump, and with reasonable HFC mode matching, optical feedback assures locking to only the fundamental HFC Gaussian mode for the pump. As expected from the HFC, high spatial quality is observed in both the transmitted pump and Stokes beams. Stokes emission is observed over a discontinuous range of 10nm by changing the resonator cavity length while holding the diode laser drive current and temperature fixed. Spectral purity of the Stokes output is expected to be limited by the acoustic stability of the HFC. The Nd:YAG-pumped cw Raman laser of reference 1, which used this cavity design, later produced an Allan variance of less than 1kHz for an integration time of 1 second [14]. We expect similar results from this system.

At higher pump powers, coherent anti-Stokes emission at 595nm is also observed. However, intensity dependent phase instabilities cause output oscillations beyond the present servo bandwidth at these higher powers. Such oscillations were overcome in the Nd:YAG

system presented in reference 2 and we expect further electronic servo bandwidth to stabilize this system at higher powers as well.

In conclusion, to our knowledge, we have demonstrated the first cw diode-pumped Raman laser. An optical feedback technique was used in concert with electronic control to stabilize the laser output at low pump powers. A laser threshold of $240 \pm 19 \mu\text{W}$ was measured indicating that the system can be pumped by inexpensive, low power diode laser sources. Anti-Stokes emission was also observed for higher, but unstable pump powers.

Acknowledgments:

This work is supported by NSF under grant # 9731602. We would also like to thank Leo Hollberg for useful discussion regarding resonant optical feedback.

References:

1. N. Bloembergen, Am. J. Phys. **35**, 989 (1967).
2. J. K. Brasseur, K. S. Repasky, and J. L. Carlsten, Opt. Lett. **23**, 367 (1998).
3. K. S. Repasky, J. K. Brasseur, L. Meng, and J. L. Carlsten, J. Opt. Soc. Am. B **15**, 1667 (1998).
4. R. Max, U. Huber, I. Abdul-Halim, J. Heppner, Y. Ni, G. Willenberg, and C. O. Weiss, IEEE J. Quantum Electron. **QE-17**, 1123 (1981).
5. M. Poelker and P. Kumar, Opt. Lett. **17**, 399 (1992).
6. S. N. Jabr, Opt. Lett. **12**, 690 (1987).
7. W. K. Bischel and M. J. Dyer, J. Opt. Soc. Am. B **3**, 677 (1986).
8. B. Dahmani, L. Hollberg, and R. Drullinger, Opt. Lett. **12**, 876 (1987).
9. Ph. Laurent, A. Clairon, and Ch. Brant, IEEE J. Quantum Electron. **QE-25**, 1131 (1989).
10. H. Li and N. B. Abraham, IEEE J. Quantum Electron. **QE-25**, 1782 (1989).
11. R. Lang, K. Kobayashi, IEEE J. Quantum Electron. **QE-16**, 347 (1980).
12. F. Favre and D. Le Guen, IEEE J. Quantum Electron. **QE-21**, 1937 (1985).
13. R. W. P. Drever, J. L. Hall, F. V. Kowalski, J. Hough, G. M. Ford, A. J. Munley, and H. Ward, Appl. Phys. B **31**, 97 (1983).
14. J. K. Brasseur, P. A. Roos, K. S. Repasky, and J. L. Carlsten, "Characterization of a continuous wave Raman laser in H₂", to be published in J. Opt. Soc. Am. B (1999).
15. K. S. Repasky, L. Meng, J. K. Brasseur, J. L. Carlsten and R. C. Swanson, "High efficiency, continuous-wave Raman lasers", to be published in J. Opt. Soc. Am. B (1999).

Figure Captions:

Figure 1: Resonant optical feedback conceptual diagram showing ring geometry. L_o is the photon travel distance outside the high finesse cavity (HFC) and L_{HFC} is the HFC mirror separation. The diode laser operating frequency is sensitive to both of these parameters. Note that energy circulates only in the clockwise direction as indicated by the arrows.

Figure 2: Diode-pumped cw Raman laser setup showing ring configuration optical locking. LD = laser diode, APP = anamorphic prism pair, GP = Glan polarizer, FR = Faraday rotator, $\lambda/2$ = half-wave plate, PBS = polarizing beam splitter, EOM = electrooptic modulator, BS = beam splitter, MML = mode matching lenses, M = mirror, PBP = Pellin-Broca prism, and HFC = high finesse cavity. Mirror M1 is reflective coated only for the pump wavelength.

Figure 3: HFC output powers for the transmitted pump at 790nm (squares) and Stokes at 1178nm (circles) as functions of input optical power. The solid lines represent theoretical models developed in references 3 and 14. The top axis gives incident pump power while the bottom axis accounts for various coupling losses into the HFC. Stokes laser threshold is observed at $240 \pm 19 \mu\text{W}$.

Figure 4: Photon conversion efficiency from the pump to the Stokes beams as a function of input optical power. The solid line represents theoretical predictions based on references 3 and 14. The top axis gives incident pump power while the bottom axis accounts for various coupling losses into the HFC. The efficiency rises throughout the pump power region studied with a peak

value of $15\pm 2\%$. The efficiency is predicted to ultimately peak at 17.5% for a pump power of 4 times threshold.

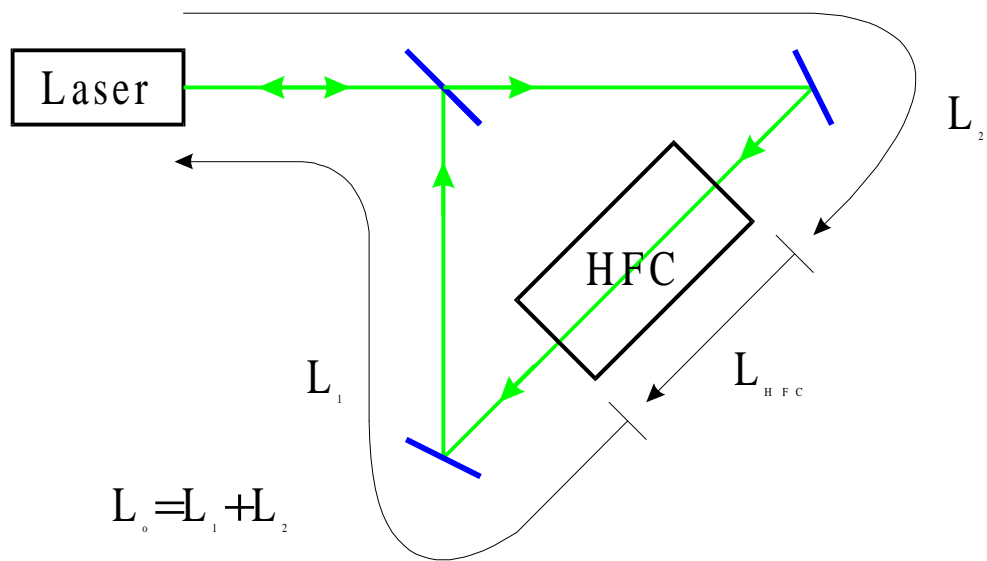


Figure 1.

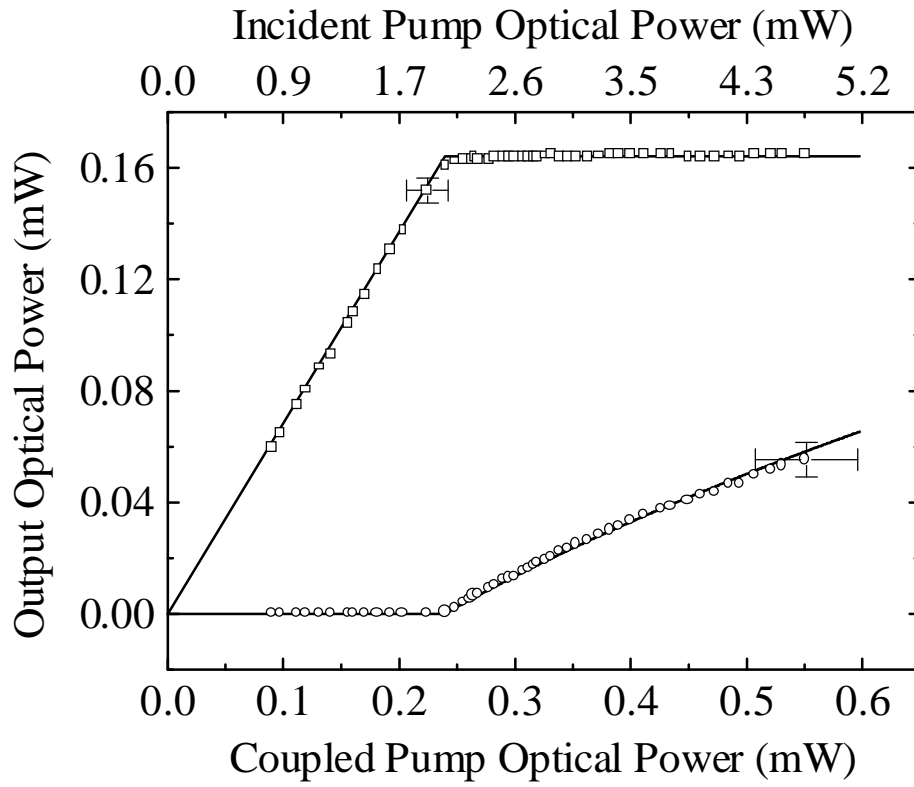


Figure 3.

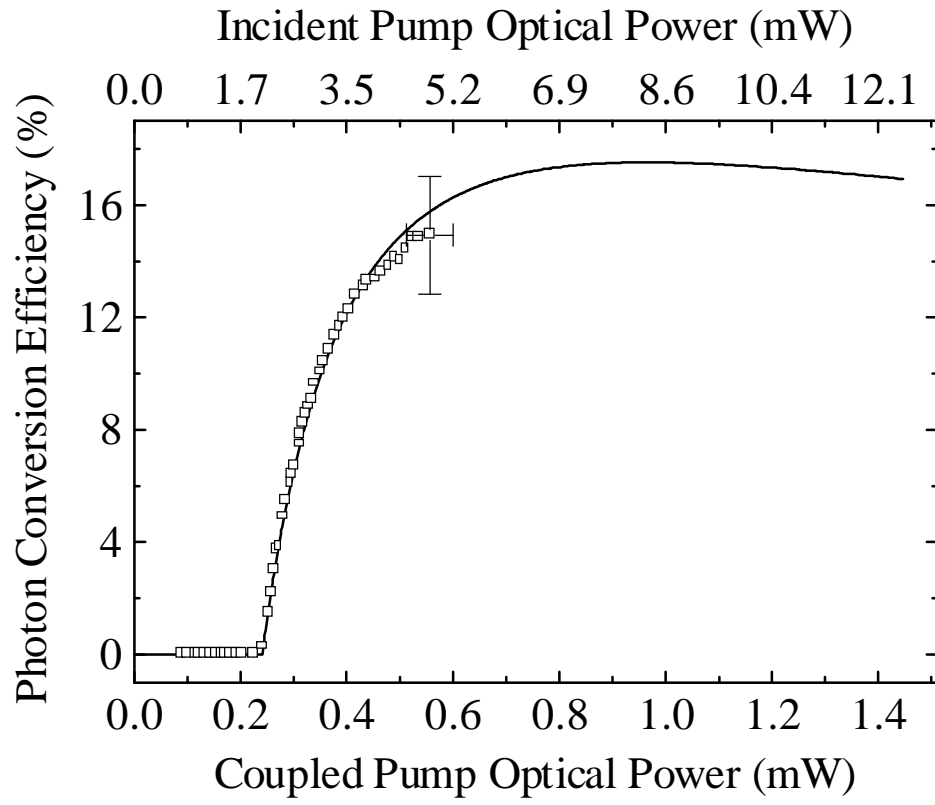


Figure 4.